Printed in the Republic of Korea
ANALYTICAL SCIENCE & TECHNOLOGY
Vol. 33 No. 2, 86-97, 2020
https://doi.org/10.5806/AST.2020.33.2.86

Study on the spectroscopic reconstruction of explosive-contaminated overlapping fingerprints using the laser-induced plasma emissions

Jun-Ho Yang and Jai-Ick Yoh★

Department of Mechanical & Aerospace Engineering, Seoul National University, 1 Gwanakro, Gwanakgu, Seoul KS013, Korea

(Received March 3, 2020; Revised April 7, 2020; Accepted April 7, 2020)

Abstract: Reconstruction and separation of explosive-contaminated overlapping fingerprints constitutes an analytical challenge of high significance in forensic sciences. Laser-induced breakdown spectroscopy (LIBS) allows real-time chemical mapping by detecting the light emissions from laser-induced plasma and can offer powerful means of fingerprint classification based on the chemical components of the sample. During recent years LIBS has been studied one of the spectroscopic techniques with larger capability for forensic sciences. However, despite of the great sensitivity, LIBS suffers from a limited detection due to difficulties in reconstruction of overlapping fingerprints. Here, the authors propose a simple, yet effective, method of using chemical mapping to separate and reconstruct the explosive-contaminated, overlapping fingerprints. A Q-switched Nd:YAG laser system (1064 nm), which allows the laser beam diameter and the area of the ablated crater to be controlled, was used to analyze the chemical compositions of eight samples of explosive-contaminated fingerprints (featuring two sample explosive and four individuals) via the LIBS. Then, the chemical validations were further performed by applying the Raman spectroscopy. The results were subjected to principal component and partial least-squares multivariate analyses, and showed the classification of contaminated fingerprints at higher than 91% accuracy. Robustness and sensitivity tests indicate that the novel method used here is effective for separating and reconstructing the overlapping fingerprints with explosive trace.

Key words: LIBS (laser-induced breakdown spectroscopy), overlapping fingerprints, trace explosives, raman spectroscopy, multivariate analysis

1. Introduction

A human fingerprint is a unique pattern of ridges in the skin of the fingertip. Owing to the presence of secretions from glands in this area, a characteristic fingerprint is frequently left on the surface of objects touched by an individual. The fingerprint pattern generally remains consistent from birth. Shape changes do occur, but the fingerprint pattern is not prone to modification by external factors, making fingerprints an effective means of identification. For example, oil imprints known as latent fingerprints

★ Corresponding author
Phone : +82-(0)2-880-1507 Fax : +82-(0)2-882-1507
E-mail : jjyoh@snu.ac.kr

are commonly gathered from crime scenes. Analyzing these is a key part of the primary investigation and may lead to the successful arrest of a suspect. Moreover, the latent fingerprint contains not only the fingertip markings but also the chemical profile of the individual. The chemical composition of a latent fingerprint differs, depending on eating habits, lifestyles, and the living environment.[1-4] For analyze the chemical composition of latent fingerprint, we utilize the laser spectroscopic technique in this paper. In laser-induced breakdown spectroscopy (LIBS), a high-intensity laser pulse is fired onto a target sample to generate plasma.[5,6] The sample absorbs energy from the laser, becoming liquefied or vaporized, depending on its initial state. Repeated laser shots are used to counter the effect of irregularity of the refractive index of focal lens, and ultimately plasma is generated. Atoms are initially excited in the irradiated region for 200 – 300 ns, and then light is emitted while returning to the ground state. The wavelength and amplitude of the light emitted during these atomic relaxations allow the atomic element present to be identified. LIBS has been utilized in a wide range of scientific applications, including forensic science, space exploration, and combustion measurement[7-12]. And, LIBS makes it possible to detect the unique chemical composition of a person's skin oil such as potassium, sodium, magnesium, iron, hydrogen, oxygen, thus providing forensic scientists with valuable additional information.[7-9]

However, it can be challenging to obtain a clean and complete fingerprint. Fingerprints found at crime scenes are often damaged, contaminated, or overlapping. Two or more overlapping fingerprints add complexity to the analysis. The traditional method of fingerprint analysis is through image processing, now generally aided by software algorithms.[13,14] Feng *et al.*[13] developed an algorithm capable of separating overlapping fingerprints by establishing the orientation of each fingerprint and reconstructing the overlapping fingerprints by measuring the vector directions of the fingerprint ridges. Stojanović *et al*.[14] took the further step of developing a technique to separate fingerprints using a neural network. However, the existing methods showed differences in results according to the user's experience or the starting point of vector analysis. Also, in case of spectroscopic method, the advantages of real-time analysis and consistency are good

Several studies[15-22] have investigated the effects of fingerprint contamination. Mou *et al*.[15] proposed attenuated reflection Fourier-transform infrared spectro-microscopy as a means of detecting and identifying explosive particles such as trinitrotolune (TNT) and trinitrobenzene (TNB) in fingerprints, whereas Lees *et al.*[16] used a simple multispectral imaging approach to investigate the chemical changes in such fingerprints. Several studies have used Raman spectroscopy to look at the effects of contamination: Ricci *et al.*[17] identified and detected marks left by fingertips contaminated by cosmetics on nonporous and porous surfaces. Exogenous material in fingerprints has been investigated through the use of adhesive lifters.[18] Contamination by explosives has also been investigated using Raman imaging, for example by Emmons *et al*.[19] In case of LIBS studies, there are analysis of single fingerprint contaminated explosives using optical catapulating-LIBS.[20-21] Lucena *et al*.[22] were successful in using standoff LIBS to investigate explosive-contaminated fingerprints from a distance. However, their study looked at non-overlapping samples, aiming at restoring a single contaminated fingerprint. The separation of explosive-contaminated overlapping fingerprint samples via LIBS has yet to be attempted. Overlapping latent fingerprints, which are left behind when the same or different individuals have touched the same object at different times, have previously been investigated from a number of perspectives.[7-9] Although challenging to analyze, such marks are an invaluable source of information when identifying suspects in a forensic investigation.

Work has also been carried out on reconstructing overlapping fingerprints via chemical means. Bradshaw *et al*.[23] developed a matrix-assisted laser desorption ionization technique that uses chemometrics to distinguish different fingerprints on the basis of chemical composition. The present authors have also used LIBS to determine the chemical compositions

of different fingerprints on the basis of the intensity of laser spectra.[7,8] These studies indicated that fingerprints are affected by the period of time they are exposed to the environment, allowing overlapping fingerprints belonging to the same person to be separated.[9]

In this work, we focus on the reconstructing the explosive-contaminated, overlapping fingerprints. The fingerprints of an individual have a chemical signature that is influenced by his or her lifestyle, while chemical analysis can further differentiate fingerprints that are left with a small time difference.[7-9] These detection efforts were limited to intact, uncontaminated overlapping fingerprints. By aiming to detect the chemical components of both the contaminating substance and the fingerprint, this study advances beyond the analyses currently reported in the literature.[7-9] We examine the effects of explosive trace on chemical profiles of the fingerprints as revealed by LIBS and Raman-derived laser spectra and determine whether overlapping samples can be reconstructed by means of multivariate analysis.

2. Experimental Setup

2.1. Fingerprint sample preparation

Overlapping, explosive-contaminated sample fingerprints were introduced onto aluminum plates as follows. To focus explosive's contamination effects, the index finger and forehead of each test subject were cleaned using 99.8 % alcohol (Sigma Aldrich) cotton swabs. Oil from the subject's forehead was then transferred to the subject's index finger by touching one to the other for about 10 s. The index finger was then pressed lightly against 25 μm fine powder explosive samples for about 5 s and then pressed onto the aluminum plate. Contaminated, overlapping fingerprints were produced by two different individuals at different times.

2.2. Preparation of explosive sample

Titanium hydride potassium perchlorate (THPP) and zirconium potassium perchlorate (ZPP) are commonly used as pyrotechnic initiators in engineering industries.[24] These materials are produced in volume and are often stored at variable temperature and humidity. The THPP mixtures, composed of TiH2, KClO4, and Viton-b (hexafluoropropene–vinylidene-fluoride copolymer), and the ZPP mixtures, composed of Zr, KClO4, graphite, and Viton-b, were both produced in powder form and were then made into a pellet to increase the clarity of the laser spectra obtained by LIBS and Raman spectroscopy. *Table* 1 summarizes the chemical compositions of the THPP and ZPP samples.

2.3. Optical setup

The LIBS system used for this study performs laser ablation and plasma generation with an internally fitted 1064-nm-wavelength Q-switched Nd:YAG laser with six-channel CCD camera (RT250-Ec, Applied Spectra Inc.) and uses a 15 × magnification

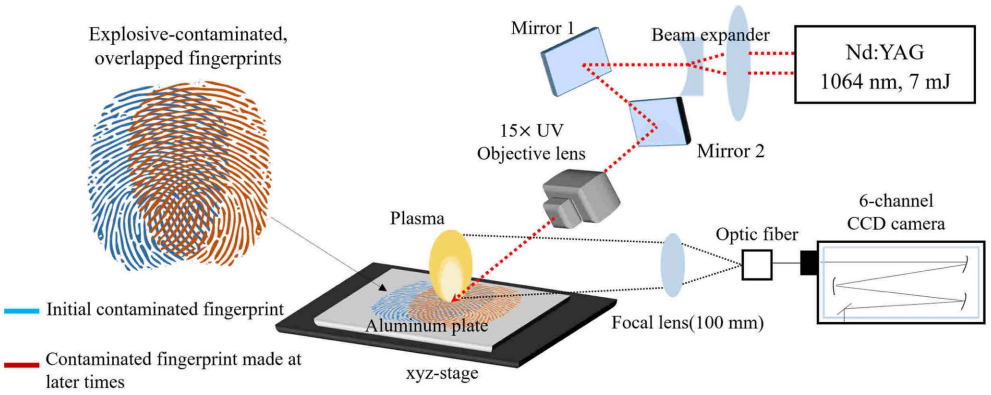

Fig. 1. Schematic of the LIBS scanning system.

objective (LMM-15X-P01, Thorlabs) to focus the laser beam. *Fig.* 1 illustrates the experimental setup. The duration of the laser pulse and the laser energy were fixed at 5 ns and 7 mJ, respectively. To minimize the size of the craters generated by laser ablation and thus increase the resolution of laser scanning, the laser energy used to generate plasma was kept to a minimum. Furthermore, a beam expander was used to minimize the beam area. The distance from the laser system to the fingerprint samples was set at 9.55 cm. The gate delay of the laser system was fixed at 1.05 us, and the laser repetition rate was set at 1 Hz. The sensor was set to detect the wavelength range 198 – 1050 nm to enable six-channel CCD spectroscopy. The spectroscopic resolution of the CCD was set at 0.1 nm for ultraviolet to visible wavelengths and at 0.12 nm for visible to near-infrared wavelengths. Laser scanning was used across the fingerprint samples to obtain the two-dimensional chemical distribution of the contaminated, overlapping fingerprints. Each laser point in the scanning process denotes the resolution of the LIBS system at a distance of 125 μm.

Raman spectroscopic technique detects the vibrational and rotational intra- or inter- motion of a molecule. When a laser beam is focused a targeted sample, part of the light is scattered by vibrations and rotations of the molecules. The degree of Raman scattering effect for each wavelength indicates the molecular structure of a targeted sample. Raman spectroscopy was also conducted using a 1064-nm-wavelength Q-switch Nd:YAG laser (Surelite 1, Continuum Inc.). The laser pulse duration was set at 5 – 7 ns, and a second-harmonic generator was used for the dominant 532-nm wavelength. A larger area was irradiated than for LIBS (<100 μm), and a laser pulse energy of 5 mJ was used so as to avoid plasma generation through laser ablation. To measure Raman scattering, the gate delay and repetition rate were set to 0 μs and 2 Hz, respectively, and the scattering signal was measured using a CCD Czerny–Turner spectrometer (MonoRA320i Andor, iStar Andor). The spectral resolution was fixed at 7 cm^{-1} from 0 to 3500 cm^{-1}, with 10-μm slits and 1200 gr/mm. The grating and gate width of the Raman system were set at 1200 grooves and 0.1 ms, respectively. A long-pass filter (LP03-532RU-25, Thorlabs) was used to remove Rayleigh-scattered light at 532 nm, and a 600-μm optical fiber was used to remove Raman-scattered light.

2.4. Multivariate analysis and data acquisition

Classification of the resulting spectra was conducted using the multivariate SIMCA (soft independent modeling by class analogy) and PLS-DA (partial least-squares discriminant analysis) methods and subjected to sensitivity (cross-validation) and robustness (validation) tests, similar to the process described in previous studies and references,[4-5,25-26] Two samples of explosives (THPP and ZPP) and four different fingerprints were prepared. One hundred and twenty sample LIBS spectra were randomly extracted from each sample condition and utilized to conduct a sensitivity test as the 30-spectrum training group and the 90-spectrum test data based on PCA and PLS result plots. Subsequently, 32 test laser spectra were constructed from four randomly chosen from 8 types of contaminated fingerprints. For the robustness test, one of the contaminated fingerprints was removed from the calibration set, and the sequence was repeated for each class. To validate the accuracy of the classification, 120 iterations were conducted independently by reselecting all the LIBS spectral data used in both the sensitivity and robustness tests. In this work, the term “correct classification” is used if the fingerprint data are classified correctly, “misclassification” if classified incorrectly, and “no classification” if no class is assigned.

Data processing was carried out using Unscrambler X 10.1 (CAMO PROCESS AS, Oslo, Norway), MATLAB R2016a software and Origin Pro 8.5.1 (Origin Lab Corporation, Northampton, MA, USA).

3. Results and Discussion

3.1. Analysis of explosive-contaminated fingerprints using LIBS

Before addressing the combined effect of contamination by explosives and overlapping fingerprints,

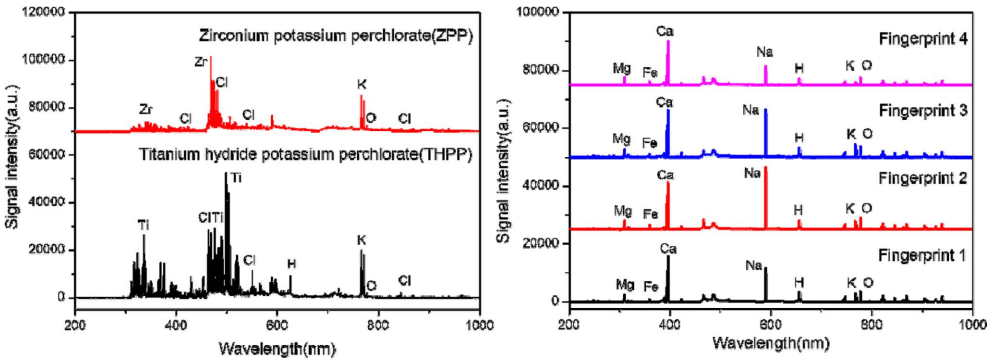

(a) (b)

Fig. 2. (a) Average LIBS spectra for explosives (THPP and ZPP), offset by 70,000 for clarity, and (b) average LIBS spectra. for latent fingerprints from four different

Table 1. Chemical composition of explosive sample

Sample	Chemical composition
THPP	32% TiH2, 63% KClO4, 5 % Viton-b
ZPP	52% Zr, 42% KClO4, 1% graphite, 5 % Viton-b

Table 2. Main emission lines from LIBS spectrum

Element	Emission lines (nm)
Mg	279.51, 285.21
K	766.49, 769.90
Na	588.91, 589.59
Ca	393.36, 396.84, 422.67
Ti	323.45, 334.90, 334.94, 363.54, 364.27, 365.35, 375.29, 498.17, 499.11, 500.99, 506.46, 521.04
H	656.28
Zr	339.19, 343.82, 349.62, 360.12, 468.78, 471.01
Cl	479.45, 542.32
Fe	238.20, 248.33, 358.12, 371.99, 373.49, 373.71

the characteristics of the LIBS- and Raman-derived laser spectra need to be identified. *Fig.* 2(a) shows the LIBS spectra of THPP and ZPP, and *Fig.* 2(b) shows the LIBS spectra of latent fingerprints collected from four individuals. One hundred points were averaged from each fingerprint so as to smooth out variability in the laser spectra. The compositions indicated by the LIBS spectra were analyzed using the NIST atomic spectra database.[27] Atomic signatures such as zirconium, titanium, chlorine, oxygen, hydrogen, and potassium were detected in the explosive samples, as would be expected given the data in *Table* 1. Atomic signatures for oxygen, hydrogen, sodium, calcium, magnesium, iron, and potassium were identified from the four latent fingerprints. Both environmental factors such as eating habits and inherent characteristics such as inherited family history and sex distinction may lead to variations in the chemical composition of the surface of the fingertip. As a result, there are minute differences in the tendency of laser spectra measured by LIBS for latent fingerprints. However, this difference in spectrum is invisible to the naked eye, and multivariate analysis is required to reconstruct a single data source where there is contamination and overlapping as is the case with these fingerprints. Relatively high signal intensities were detected at wavelengths of approximately 279, 285, 358, 371, 373, 393, 396, 588, 589, 656, 766, and 777 nm in the fingerprint spectra (*Table* 2). These were interpreted as LIBS signals for Mg, Fe, Ca, O, K, and Na, as shown in *Fig.* 2(b).

Fig. 3 shows the LIBS spectra of explosive-contaminated fingerprints, confirming the presence of traces of explosives in the signals. A peak corresponding to the signal from THPP, namely titanium, can be seen *in Fig.* 3(a), but its intensity is relatively small compared with the overall laser spectrum. The calcium and potassium peaks are comparatively higher. The ZPP explosive spectrum shows no peaks corresponding to the sodium and hydrogen signals,

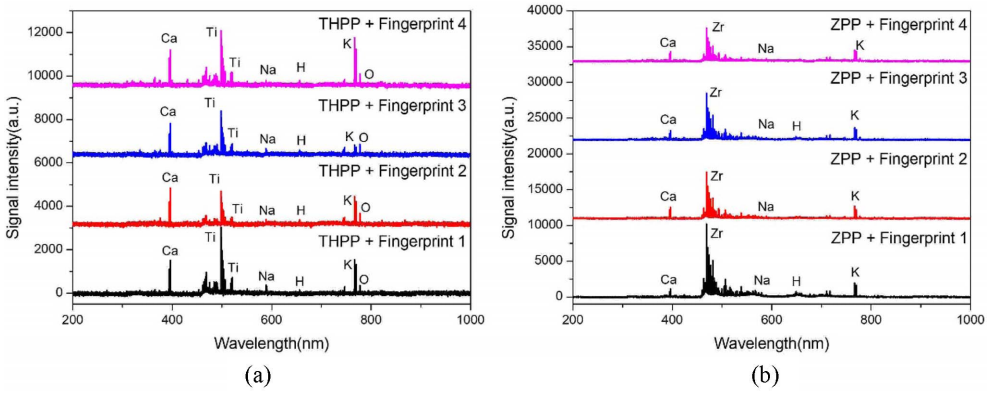

Fig. 3. Average LIBS spectra for explosive-contaminated fingerprints, (a) THPP + fingerprints, (b) ZPP + fingerprints.

allowing the zirconium signal to be detected simultaneously with fingerprint-specific elements (*Fig.* 3(b)). These distinctions allow useful atomic data to be obtained when the explosive residues and latent fingerprints are ablated and converted to plasma together.

3.2. Validation of LIBS results via Raman spectroscopy

Raman spectroscopy is used to measure the vibrational and rotational motion of a molecule that results from inter- or intramolecular interactions. Raman scattering is typically weaker than Rayleigh scattering, but the use of a notch filter allows Rayleigh-scattered light to be separated from inelastically scattered light. When a laser beam irradiates the targeted sample, some of the photons change their energy state as a result of interaction with the sample, depending on the vibrational and rotational modes of the molecules that they encounter. The amplitude and wavelength of this Raman scattering indicate the molecular structure and chemical composition of the targeted sample. Because Raman spectroscopy and LIBS use the same optics[28], Raman spectroscopy data can be used to complement and validate LIBS data.

Figs. 4(a) and 4(b) shows the spectra of the explosive samples and four different latent fingerprints as obtained by Raman spectroscopy. The Raman signal was obtained by summing 30 laser spectra, and the average values of 10 Raman signals were used in the plots for reliability. *Table* 3 summarizes the main Raman emission lines. ZPP and THPP have similar Raman signals because of the high proportion of $KClO_4$ within both. The presence of this molecule is revealed by the relatively high-intensity signals at Raman shifts of 939.75, 458.47, 630.26, 1079.37, and 1114.12.[29] THPP differs from ZPP in that it contains TiH_2, but this is not apparent in the Raman signal. Both explosives allow for the minute fluore- scence signal to be detected. The Raman signal of the latent fingerprints reveals the existence of glycine, serine, acetic acid, aspartic acid, pyruvic acid, lactic acid, and CN bonds,[5] as shown in *Table* 3.

Table 3. Main Raman scattering emission lines for explosives and latent fingerprint

Element	Emission line (1/cm)
KClO4	450-470, 620-650, 900-940
CN	1610-1665 (double), 2249 (triple)
Isobutyric acid	800, 1100
Acetic acid	800, 1100
Aspartic acid	~1475-1580
Serine	550
Lactic acid	~1475-1580
Pyruvic acid	~1475-1580
Glycine	1670

Figs. 4(c) and 4(d) show the Raman spectra of contaminated fingerprints from 200 to 3200 cm^{-1}.

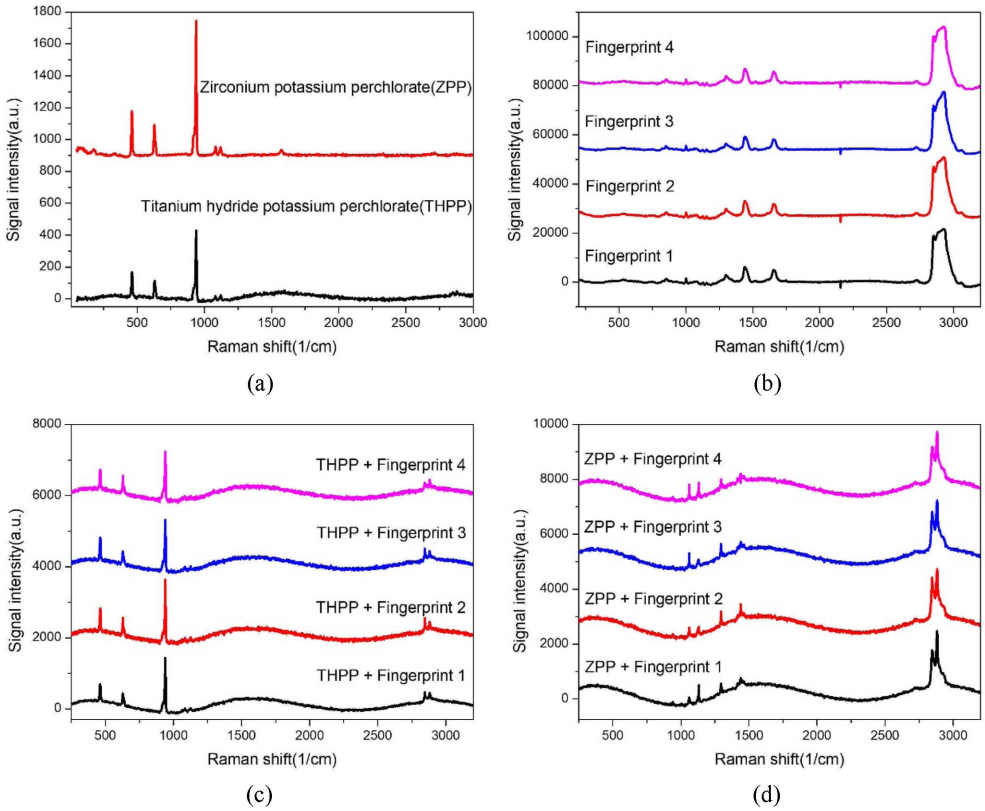

Fig. 4. Average Raman spectra for (a) explosives, (b) latent fingerprints from four different individuals, (c) explosive (THPP) contaminated fingerprints, and (d) explosive (ZPP) contaminated fingerprints.

The laser spectra show mixing of the signals of the contamination and the fingertips, with peaks in signal intensity attributable to amino acids, fatty acids, oils, the $KClO_4$ signal, and the fluorescence signal due to the explosives. Thus, Raman spectroscopy further confirms that the presence of traces of explosives changes the chemical composition of latent fingerprints and changes the laser spectrum as a result.

3.3. Multivariate analysis for the effect of contamination by explosives

Fig. 5(a) is a PCA loading plot derived from principal component analysis (PCA) of the data obtained from four different explosive-contaminated fingerprints. 120 LIBS spectral data for each contaminated fingerprint were classified. It can be seen that higher than 90 % of the total spectral data is explained when applying only PC 1 and PC 2. Each contaminated fingerprint lies in an independent region; measurements corresponding to different explosives are grouped within these regions. The same applies to PLS results, as shown in *Fig.* 5(c). This suggests that classification methods such as SIMCA and PLS-DA can be used to identify the type of explosives present and to distinguish the origin of latent fingerprints and so extract the composition of fingerprints and explosives independently from LIBS spectra. Furthermore, depending on the type of explosives present and the origin of the fingerprints, the distinctions seen in the PCA and PLS plots may enable precise classification.

These inferences were tested by assessing the sensitivity and robustness of classification and the reconstruction of contaminated, overlapping fingerprints following the procedure outlined in references.[3-5,25,26]

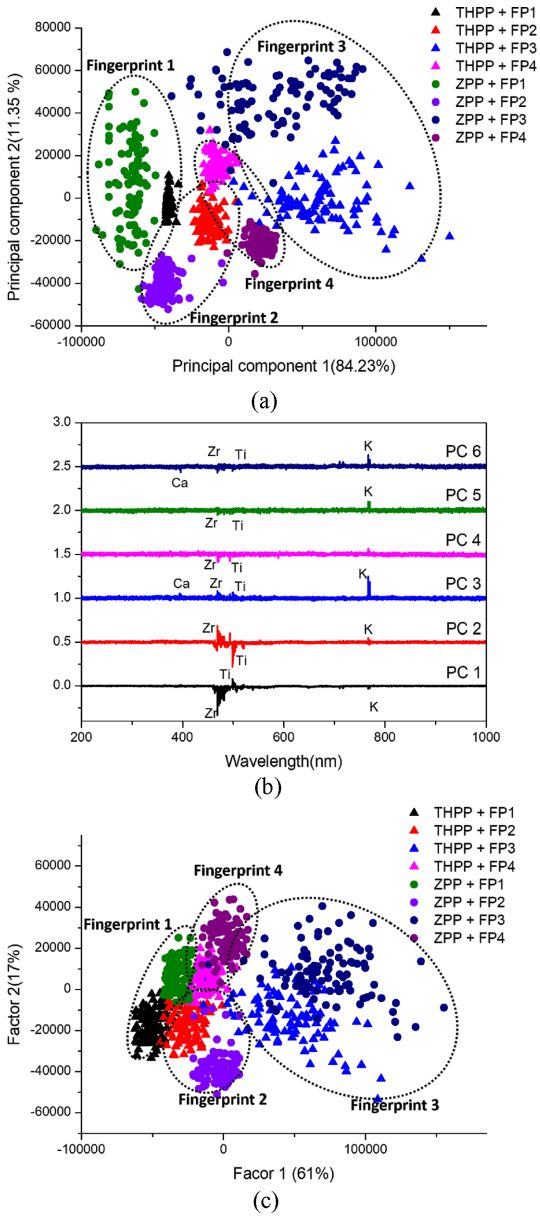

Fig. 5. (a) PCA of LIBS spectrum, (b) extracted PCs, and (c) PLS analysis of LIBS spectrum.

When applying these to SIMCA classification, both the results of SIMCA classification of the overall data and the random spectra extracted from the contaminated fingerprint data were used to ensure statistical reliability, which was further increased by conducting 120 iterations. The distinction between a sensitivity test and a robustness test is whether the test sample is extracted from the first set of 120 fingerprint data or from the additional extracted laser spectra. The results are summarized in *Table* 4. In the sensitivity test, on average 95.75 % were categorized accurately, 2.50 % were inadequate, and 1.75 % were not classified. In the robustness test, these figures were 91.40 %, 4.83 %, and 3.76 %, respectively. The robustness result, yielding an accuracy of 91 % or more, confirms that it is possible to classify and distinguish the source and origin of contaminated fingerprints using SIMCA. The chemical compositions of different fingerprints can be reconstructed and separated by determining the chemical composition of the contaminated, overlapping latent fingerprints.

For analysis of PLS-DA, similarly, the same laser spectral data were applied to the eight contaminated fingerprints, after which PLS regression was performed on each type. Although PLS-DA classification is theoretically more stable and robust than SIMCA analysis, the results shown in *Tables* 4 and 5 are not significantly distinct from the SIMCA results. In the sensitivity test, 94.88 % were correctly classified, misclassification was at 2.11 %, and no classification was at 3.0 %, indicating a relatively higher accuracy for PLS-DA analysis than for SIMCA analysis: there is a small drop in the probability of mis- or no classification. The probabilities of correct-, mis-, and no classification in the robustness experiment were found to be 91.10 %, 3.65 %, and 5.25 %, respectively. This indicates a lower average accuracy than in SIMCA and a higher probability of misclassification. However, the probability of no classification by SIMCA was higher. Relatively, in the case of PLS-DA, results have a higher unclassified rate. Because for this application a false identification is worse than no identification.

3.4. Separation of overlapping fingerprints with traces of explosive

The results presented in the previous section show that SIMCA and PLS-DA can be used to accurately classify the explosive elements found on latent fingerprints and the sources of those fingerprints simultaneously. This indicates the usefulness of

Table 4. Classification probability using SIMCA

(a) Sensitivity test			
Type	Correct classification	Misclassification	No classification
THPP + Fingerprint 1	0.9210	0.0340	0.0450
THPP + Fingerprint 2	0.9327	0.0373	0.3000
THPP + Fingerprint 3	0.9750	0.0000	0.0250
THPP + Fingerprint 4	0.9260	0.0670	0.0070
ZPP + Fingerprint 1	0.9870	0.0130	0.0000
ZPP + Fingerprint 2	1.0000	0.0000	0.0000
ZPP + Fingerprint 3	0.9850	0.0150	0.0000
ZPP + Fingerprint 4	0.9333	0.0333	0.0333
(b) Robustness test			
Type	Correct classification	Misclassification	No classification
THPP + Fingerprint 1	0.8750	0.1000	0.0250
THPP + Fingerprint 2	0.9010	0.0670	0.0320
THPP + Fingerprint 3	0.9220	0.0290	0.0490
THPP + Fingerprint 4	0.8933	0.0450	0.0617
ZPP + Fingerprint 1	0.9333	0.0333	0.0333
ZPP + Fingerprint 2	0.9270	0.0160	0.0570
ZPP + Fingerprint 3	0.9250	0.0440	0.0310
ZPP + Fingerprint 4	0.9360	0.0520	0.0120

Table 5. Classification probability using PLS-DA

(a) Sensitivity test			
Type	Correct classification	Misclassification	No classification
THPP + Fingerprint 1	0.9450	0.0300	0.0250
THPP + Fingerprint 2	0.9360	0.0260	0.0380
THPP + Fingerprint 3	0.9446	0.0333	0.0221
THPP + Fingerprint 4	0.9333	0.0333	0.0333
ZPP + Fingerprint 1	0.9650	0.0000	0.0350
ZPP + Fingerprint 2	0.9467	0.0233	0.0300
ZPP + Fingerprint 3	0.9540	0.0233	0.0227
ZPP + Fingerprint 4	0.9660	0.0000	0.0340
(b) Robustness test			
Type	Correct classification	Misclassification	No classification
THPP + Fingerprint 1	0.9150	0.0300	0.0550
THPP + Fingerprint 2	0.9077	0.0233	0.0700
THPP + Fingerprint 3	0.9140	0.0707	0.0153
THPP + Fingerprint 4	0.9170	0.0303	0.0527
ZPP + Fingerprint 1	0.8988	0.0233	0.0779
ZPP + Fingerprint 2	0.9055	0.0277	0.0668
ZPP + Fingerprint 3	0.9144	0.0656	0.0200
ZPP + Fingerprint 4	0.9160	0.0220	0.0620

multivariate analysis for distinguishing and separating the contaminated, overlapping fingerprints. To form prediction classes for PCA and PLS, 50 laser spectra were first extracted from each of the eight types of

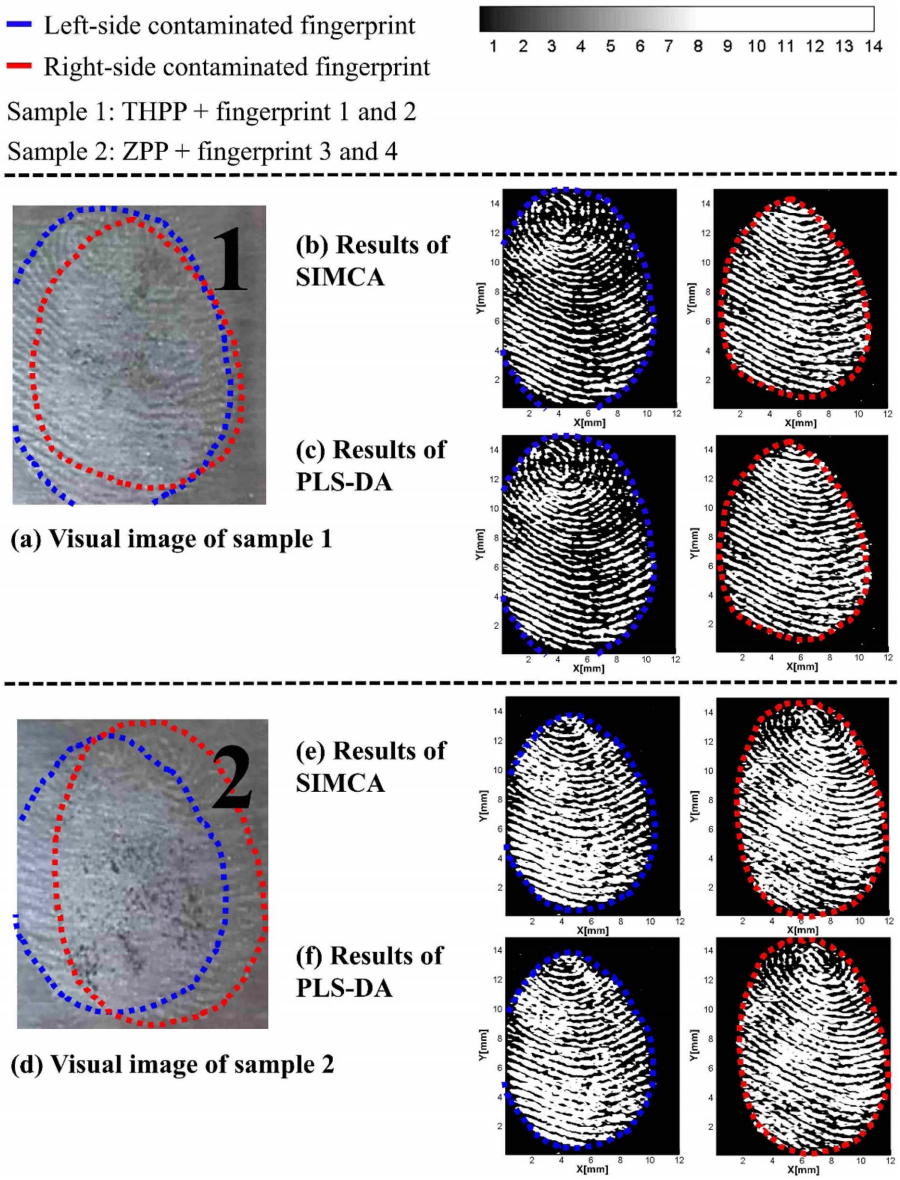

Fig 6. Reconstruction of overlapping fingerprints contaminated by the same explosives.

contaminated fingerprints. The laser spectrum data for each laser point on a contaminated sample were then transformed into multivariate data, and the abovementioned classification sequence was applied to these PCA and PLS plots. Each spectrum corresponds to an individual position in the sample, and the lateral resolution of the LIBS scan was 125 μm. Also, there exists no overlapping between points. Latent fingerprints, explosives, and fingerprints contaminated by explosives were classified, and the contaminated, overlapping fingerprints were successfully reconstructed via multivariate analysis in several cases, as illustrated in *Figs.* 6 and 7.

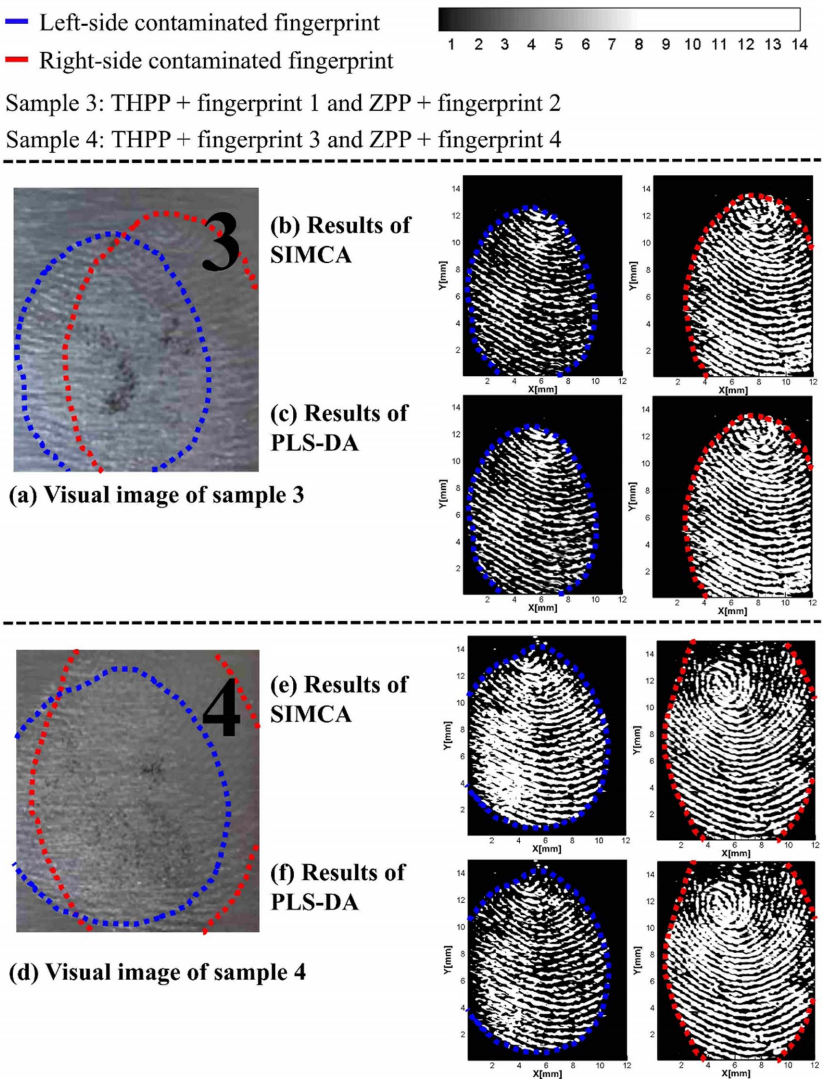

Fig. 7. Reconstruction of overlapping fingerprints contaminated by different explosives.

4. Conclusions

In this paper, the possibility of chemical mapping by LIBS combined with chemometrics provides a promising alternative in terms of separation of explosive-contaminated, overlapping fingerprints. Residues from latent fingerprint of two explosives have been successfully detected from the LIBS and Raman spectroscopy. It was found that contamination by explosive powders causes a change in chemical composition at the latent fingerprint surface. However, the chemical properties of explosives and fingerprints do not disappear. Based on this findings, the explosive-contaminated fingerprints were then classified using chemometric methods, specifically SIMCA and PLS-DA. A more exhaustive classification was carried out by using a SIMCA and PLS-DA based in the peak intensity ratios that allowed an identification of the explosives and fingerprints. As mentioned, extraction of chemical features from LIBS data suggests that can be used for constructing a concise classifier for the distribution of both explosives and latent

fingerprints. The independent position of each fingerprint and of examples contaminated by different explosives on PCA and PLS plots resulting from these analyses indicates that classification of contaminated fingerprints is possible. Finally, this confirms that explosive-contaminated, overlapping fingerprints can be separated on the basis of two-dimensional chemical distribution. Furthermore, the reported results, with error percentages not higher than 10 %, validate the suitability of the algorithm for reconstruct contaminated, overlapping fingerprints commonly applied.

Acknowledgements

This research was also supported by the Basic Science Research Program through the National Research Foundation of Korea (NRF) funded by the Ministry of Education (NRF-2016R1D1A1A02937421).

References

1. N. E. Archer, Y. Charles, J. A. Elliott and S. Jickellss, *Forensic Sci. Int.,* **154**(2), 224-239 (2005).
2. R. S. Croxton, M. G. Baron, D. Butler, T. Kent and V. G. Searss, *Forensic Sci. Int.,* **199**(1), 93-102 (2010).
3. K. M. Antoine, S. Mortazavi, A. D. Miller and L. M. Millers, *J. Forensic Sci.*, **55**(2), 513-518 (2010).
4. A. Johnston and K. Rogers, *Appl. Spectrosc.*, **71**(9), 2102-2110 (2017).
5. L. J. Radziemski, *Spectrochim. Acta, Part B.,* **57**(7), 1109-1113 (2002).
6. D. W. Hahn and N. Omenetto, *Appl. Spectrosc.*, **66**(4), 347-419 (2012).
7. J.-H. Yang, S.-J. Choi and J. J. Yoh, *Spectrochim. Acta, Part B.,* **134**, 25-32 (2017).
8. J.-H. Yang and J. J. Yoh, *Appl. Spectrosc.,* **72**(7), 1047-1056 (2018).
9. J.-H. Yang and J. J. Yoh, *Microchem. J.,* **139**, 386-393 (2018).
10. K.-J. Lee, S.-J. Choi and J. J. Yoh, *Spectrochim. Acta, Part B.*, **101**, 335-341 (2014).
11. S. H. Lee, H. Do and J. J. Yoh, *Combust. Flame.*, **165**, 334-345 (2016).
12. S. Choi and J. J. Yoh, *Spectrochim. Acta, Part B.*, **134,** 75-80 (2017).
13. J. Feng, Y. Shi and J. Zhou, *IEEE Trans Information Forensic and Security*, **7**(5), 1498-1510 (2012).
14. B. Stojanović, A. Nešković and O. Marques, *Multimedia Tools and Applications,* **76**(10), 12775-12799 (2017).
15. Y. Mou and J. M. Rabalais, *J. Forensic Sci.,* **54**(4), 846-850 (2009).
16. H. Lees, F. Zapata, M. Vaher and C. Garcia-Ruiz, *Talanta*, **184**, 437-445 (2018).
17. C. Ricci and S. G. Kazarian, *Surf. Interface Anal.,* **42**(5), 386-392 (2010).
18. M. J. West and M. J. Went, *Forensic Sci. Int.*, **174**(1), 1-5 (2018).
19. E. D. Emmons, A. Tripathi, J. A. Guicheteau, S. D. Christesen and A. W. Fountain, *Appl. Spectrosc.*, **63**(11), 1197-1203 (2009).
20. M. Abdelhamid, F. Fortes, M. Harith and J. Lasernas, *J. Anal. At. Spectrom.*, **26**(7), 1445-1450 (2010).
21. M. Abdelhamid, F. Fortes, J. Laserna and M. Harith, *AIP Conference Proceedings*, 55-59 (2011).
22. P. Lucena, I. Gaona, J. Moros and J. J. Laserna, *Spectrochim. Acta, Part B.,* **85**, 71-77 (2013).
23. R. Bradshaw, W. Rao, R. Wolstenholme, M. R. Clench, S. Bleay and S. Francese, *Forensic Sci. Int.*, **222**(13), 318-26 (2012).
24. Z. Baber and A. Q. Malik, *Fire Mater.*, **41**(2), 131-141 (2017).
25. N. C. Dingari, I. Barman, A. K. Myakalwar, S. P. Tewari and M. K. Gundawars, *Anal. Chem.,* **84**(6), 2686-2694 (2012).
26. S. Laville, M. Sabsabi and F. R. Doucet, *Spectrochim. Acta, Part B.*, **62**(12), 1557-1566 (2017).
27. A. Kramida, Y. Ralchenko and J. Reader, 'NIST atomic spectra database (ver. 5.2)', 2015.
28. S. Choi, D. Kim, J. Yang and J. J. Yoh, *Appl. Spectrosc.* **71**(4), 678-685 (2017).
29. N. Toupry, H. Poulet, M. Le Postollec, R. M. Pick and M. Yvinec, *J. Raman Spectrosc.,* **14**(3), 166-177 (1983).

Authors' Position

Jun-Ho Yang : Graduate student

Jai-Ick Yoh: Professor